DOI: 10.1002/cmdc.200700189

Molecular Models of the Interface between Anterior Pharynx-Defective Protein 1 (APH-1) and Presenilin Involving GxxxG Motifs

Krzysztof Jozwiak,[a, b] Krystiana A. Krzysko,[a] Lukasz Bojarski,[a] Magdalena Gacia,[c] and Slawomir Filipek*[a]

γ-Secretase is an integral membrane protease, which is a complex of four membrane proteins. Improper functioning of γ-secretase was found to be critical in the pathogenesis of Alzheimer's disease. Despite numerous efforts, the structure of the protease as well as its proteolytic mechanism remains poorly understood. In this work we constructed a model of interactions between two proteins forming γ-secretase: APH-1 and presenilin. This interface is based on a highly conserved GxxxGxxxG motif in the APH-1 protein. It can form a tight contact with a small-residue AxxxAxxxG motif in presenilin. Here, four binding modes based on similar structures involving GxxxG motifs in glycophorin and aquaporin were proposed and verified. The resulting best model employs antiparallel orientations of interacting helices and is in agreement with the currently accepted topology of both proteins. This model can be used for further structural characterization of γ-secretase and its components.

Introduction

Alzheimer's disease (AD), the most common form of dementia in the elderly, is characterized by accumulation of β-amyloid (Aβ) senile plaques in the brain. Aβ is produced by a cascade of proteolytic cleavages of amyloid precursor protein (APP), and the last cut is performed by γ-secretase. The failure of Aβ clearance, or mutations in APP or in γ-secretase lead to the pathological aggregation of this peptide.[1–3]

γ-Secretase is an integral membrane enzymatic complex that contains four protein entities: presenilin (PS), anterior pharynx-defective protein 1 (APH-1), nicastrin (NCT) and presenilin enhancer protein 2 (PEN-2). The exact stoichiometry of the components seems to vary depending on the development and maturation of the complex.[4] Simultaneous overexpression of these four proteins reconstitutes modest γ-secretase activity in yeast, *Drosophila*, and mammalian cells.[5–7] Apart from these crucial proteins, others that may modulate γ-secretase activity were also found.[8]

Of the γ-secretase components, only NCT is a single-span transmembrane protein that contains a massive extramembrane domain; the other components span the bilayer several times and are predominantly buried within the membrane. Thus, the γ-secretase complex residing in the bilayer has relatively small extramembrane domains.[9] A proposed model[7] of stepwise assembly suggests that the nascent PS holoprotein is stabilized in an inactive complex by binding to APH-1 and NCT. In the next step PEN-2 binds to this complex and facilitates endoproteolysis of PS into N- and C-terminal fragments (NTF and CTF, respectively), which in turn induces γ-secretase proteolytic activity.

Presenilins (PS-1 and PS-2) provide two aspartic acid residues located within the membrane to form a catalytic core for the intramembrane proteolysis of substrates. The first (D257 in PS-1 and D263 in PS-2) is preceded by an evolutionarily conserved tyrosine residue, and the second (D385 in PS-1 and D366 in PS-2) is a part of a larger GxGD motif necessary for catalytic activity. Genetic studies have shown that more than 100 mutations in the PS-1 protein are associated with familial forms of Alzheimer's disease (FAD), and new mutations are still being identified.[10] These pathogenic mutations lead to an overproduction of highly aggregative forms of Aβ within the brain. A vast majority of PS-1 mutations occur within the transmembrane regions indicating that even minute changes in the structure of these regions may radically change properties of the protein including its catalytic characteristics.[10,11] Residues associated with these pathological mutations appear to form vertical patterns along the helices when mapped on regular α helices.[12] Recently, Jozwiak et al.[13] used these linear patterns of FAD mutations as a guide to propose conceptual models of PS-1 membrane helical bundles.

Despite concerted efforts, the molecular structure of presenilins is still unknown. Even their membrane topology is a matter of controversy. Several putative topologies of PS-1 are in current discussion, including some with six or eight transmembrane helices (TMs) with a cytoplasmic location of the N terminus and two 7-TM topologies, in which the N-terminal

[a] *Dr. K. Jozwiak, K. A. Krzysko, L. Bojarski, Dr. S. Filipek*
International Institute of Molecular and Cell Biology
4 Ks. Trojdena St., 02-109 Warsaw (Poland)
Fax: (+48) 22-5970715
E-mail: sfilipek@iimcb.gov.pl

[b] *Dr. K. Jozwiak*
Department of Chemistry, Medical University of Lublin
4 Staszica St., 20-081 Lublin (Poland)

[c] *M. Gacia*
Medical Research Center, Polish Academy of Sciences
5 Pawinskiego St., 02-106 Warsaw (Poland)

end is located on the cytoplasmic side or on the extracellular side of the membrane (reviewed in [14]). However, recent data based on different experimental approaches suggest a 9-TM topology.[15–17]

In contrast to PS, the topology of APH-1 is experimentally well determined. It contains seven membrane-spanning helices with a topology essentially identical to many other well-studied 7-TM proteins.[18] The APH-1 protein is involved in the stabilization of the γ-secretase complex, although its precise role remains unknown.[19] This protein contains tandem GxxxG motifs within its fourth transmembrane domain (TM4). Substitution of the first glycine residue of this motif is associated with the loss-of-function phenotype (anterior pharynx-defective phenotype) in *C. elegans*.[20] Further studies have shown that certain mutations of the two other glycine residues impair the function of γ-secretase.[21,22] These observations allowed Lee et al. to suggest that the GxxxGxxxG motif is essential for helix–helix interaction during formation of the complex.[22] These authors postulated that A118, a small residue located one turn before the glycine motif on the α helix, could additionally reinforce the postulated helix–helix interactions. Thus, the APH-1 helical motif can be extended as follows: (A118)xxxGxxxGxxx(G130).[22] Interaction with other protein components of γ-secretase as well as the fact that APH-1, similarly to PS, undergoes endoproteolysis,[18] unquestionably affects its structural organization.

The goals of the work presented herein were to explore the structure and function of the GxxxGxxxG motif of APH-1 located on TM4 and to suggest a possible molecular mechanism of interaction with the partner helix in the γ-secretase complex. Molecular modeling techniques were used to build four alternative molecular models of helix–helix interaction involving this motif of APH-1, and the most probable model was chosen. Genotyping of FAD patients was performed in order to identify any mutation/polymorphism in the studied region of APH-1 TM4.

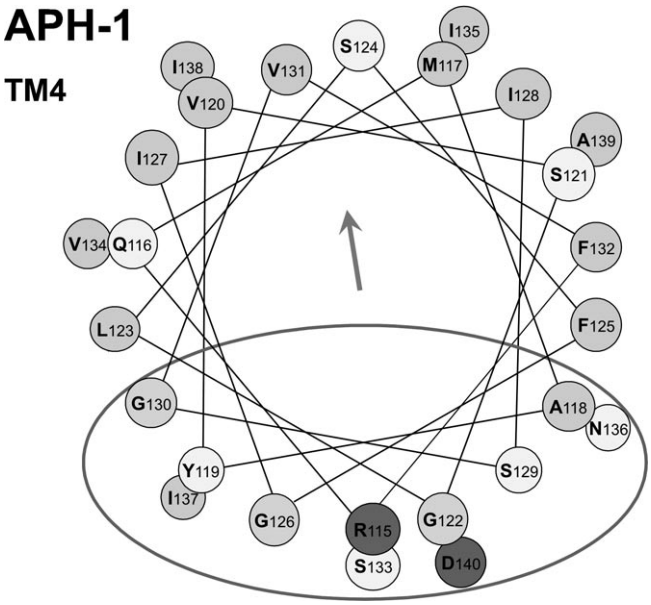

Figure 1. The helical wheel showing locations of amino acid residues along the APH-1 TM4 α helix. The red ellipse encircles residues that form the contact surface for the postulated helix–helix interactions. An arrow in the middle of the wheel shows the direction of the 'lipole' moment of the helix. The figure was generated using the MPEx v. 2.2a software.[36]

Results

The putative GxxxG interface of APH-1

The small-residue motif (G122)xxx(G126)xxx(G130) located on TM4 of APH-1 is accompanied by other residues. Mapping the sequence of APH-1 TM4 over the α helix frame revealed that the following residues are located on one face of the helix: R115, A118/Y119, G122, G126, S129/G130, S133, N136/I137 and D140 (Figure 1). Assuming that TM4 spans 26 amino acids (7 helical turns), all the aforementioned residues form a linear arrangement that may serve as an interface for possible interactions. An additional observation from the analysis of the helical wheel (Figure 1) is that the two charged residues which border the lipophilic region at both ends, R115 and D140, are located on the same side of the helix and virtually on the same face as the important G122 residue. An analysis of lipophilicity distribution shows that such a helix carries a significant 'lipole' moment (name analogous to dipole moment) oriented in the opposite direction from the interface containing three glycine residues (Figure 1).

Comparison of sequences of the TM4 segment of the APH-1 protein originating from different species (Figure 2) reveals that all residues postulated to form the helical surface for helix–helix interactions are highly conserved. A limited number of conserved polymorphisms occur only at R115, I137 and D140. Such features strongly support the hypothesis that all residues identified as forming the interface play a key role in the functioning of APH-1.

		115			118	119			122				126			129	130			133			136	137			140	
Hs	APH-1a	I	**R**	Q	M	**A**	**Y**	V	S	**G**	L	S	F	**G**	I	I	**S**	**G**	V	F	**S**	V	I	**N**	**I**	L	A	**D**	A
Hs	APH-1b	M	**R**	L	L	**A**	**Y**	V	S	**G**	L	G	F	**G**	I	M	**S**	**G**	V	F	**S**	F	V	**N**	**T**	L	S	**D**	S
Mm	APH-1a	I	**R**	Q	M	**A**	**Y**	V	S	**G**	L	S	F	**G**	I	I	**S**	**G**	V	F	**S**	V	I	**N**	**I**	L	A	**D**	A
Mm	APH-1b/c	M	**R**	L	L	**A**	**Y**	V	S	**G**	L	G	F	**G**	I	M	**S**	**G**	V	F	**S**	F	V	**N**	**T**	L	S	**N**	S
Rn	APH-1a	I	**R**	Q	M	**A**	**Y**	V	S	**G**	L	S	F	**G**	I	I	**S**	**G**	V	F	**S**	V	I	**N**	**I**	L	A	**D**	A
Dr	APH-1b	M	**R**	Q	L	**A**	**Y**	V	S	**G**	L	G	F	**G**	F	M	**S**	**G**	A	F	**S**	V	V	**N**	**I**	L	S	**D**	S
Gg	APH-1	L	**K**	Q	M	**A**	**Y**	V	S	**G**	L	S	F	**G**	I	I	**S**	**G**	V	F	**S**	V	I	**N**	**I**	L	A	**D**	S

Figure 2. Comparison of sequences involved in the formation of the TM4 segment in the APH-1 protein across species. Residues bolded and in gray boxes point in the same direction as those encircled on the helical wheel of Figure 1. Sources of sequences: Hs (*Homo sapiens*) APH-1a [NCBI:AAH15568], Hs APH-1b [NCBI:AAH20905], Mm (*Mus musculus*) APH-1a [NCBI:AAH57865], Mm APH-1b [NCBI:AAH50923], Rn (*Rattus norvegicus*) APH-1a (predicted) [NCBI:BC087081], Dr (*Drosophila melanogaster*) APH-1b [NCBI:NP_956409], Gg (*Gallus gallus*) APH-1a (predicted) [NCBI:XP_429030].

APH-1 TM4 genotyping in patients with FAD

The contribution of sequence variation in the *APH1a* gene fragment corresponding to the TM4 domain to FAD development was investigated on a group of Polish FAD patients. We screened the DNA fragment of the *APH1a* gene corresponding to TM4 in 55 patients with FAD. No changes in the analyzed DNA fragment were found. These results are in agreement with data concerning sporadic Alzheimer's disease (SAD) in the Italian population.[23]

Possible partner helices for the APH-1 interface

In the next step, the investigations were focused on finding the helix containing a motif complementary to GxxxGxxxG in TM4 of APH-1. Such complementarity would require the involvement of a similar Gly motif to form very close contacts between interacting helices. In order to identify sequence fragments containing small residues (Gly, Ala, or Ser) separated by the distance of three other residues and located within TMs, we searched sequences of other components of γ-secretase. Such motifs were found in neither PEN-2 nor NCT proteins, indicating that a partner helix of the GxxxGxxxG motif in TM4 of APH-1 was likely to be found in PS-1.

Six hydrophobic regions (HRs) of PS-1 NTF, assumed to be TMs in all published topologies of PS-1, do not carry any motifs that meet the sequence criteria described above. On the other hand, three such motifs can be found in the PS-1 CTF. The first one, (**G**378)VKL**G**LG(D385) is present in HR8. It contains an aspartic acid residue in position 385, which is involved in the formation of the catalytic core of the protease. It seems unreasonable to expect that this part of the HR8 helix interacts closely with the APH-1 protein. It is very likely, however, that the identified GxxxG motif of PS-1 HR8 is essential for tight packing interactions with the substrate protein APP (APP contains three (small)xxx(small) motifs within its transmembrane domain).

The next helix of PS-1 that carries a complementary motif for interaction with APH-1 is HR9. This region contains the sequence (**A**409)CFV**A**LI(**G**417). Such a motif of small residues, each separated by three other residues, would facilitate the formation of an interface with the complementary motif in APH-1 TM4 analogously to interactions in the transmembrane helix dimer of glycophorin A (GpA) or other systems.[24,25]

Another region of PS-1 that might possibly form a complementary motif of small residues is located in HR10. The sequence (A431)LP**A**LPI**S**ITF(**G**442) contains Ala, Ser, and Gly residues separated by three other residues. This highly evolutionarily conserved region contains a PAL motif common to all intramembrane-cleaving aspartic proteases (presenilins and its analogues, signal peptide peptidase, and others).[2] Therefore, HR10 does not seem suitable to form an interface to bind APH-1.

Models of the APH-1–PS-1 interface based on GpA

Homology/comparative modeling with subsequent structure optimization methods were employed to develop models of the interface between the helices of HR9 in PS-1 and TM4 in APH-1. The most thoroughly investigated intramembrane interaction mediated by a GxxxG motif is that which occurs in dimers of GpA. In the most plausible alignment of PS-1 HR9 and APH-1 TM4 sequences over the GpA template (shown in Figure 3), both glycine residues are followed by hydrophobic and branched valine residues, which were determined to be very important for proper van der Waals interactions providing a conformationally restricted interface between helices.[26] In our model of interactions, corresponding Gly or Ala residues of APH-1 TM4 or PS-1 HR9 are followed by either Leu or Ile (Figure 3). These residues meet the same criteria as valine (branched and hydrophobic), which suggests that the same type of helix–helix interaction is plausible.

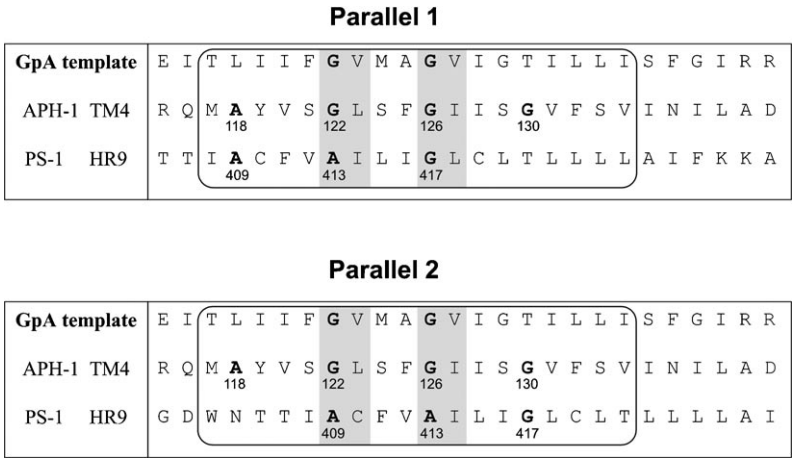

Figure 3. Two alignments of APH-1 TM4 and PS-1 HR9 using the template sequence of GpA dimer. Rounded squares mark the sequence area in the modeled helices. These areas were used to calculate interaction energies and contact surface areas. Grey boxes denote the most important residues for alignment.

The crystal structure of the dimer of transmembrane helices of GpA is known (PDB code: 1AFO).[25] Thus, we used this structure as a template to generate an approximate model of the interaction between PS-1 HR9 and APH-1 TM4. Subsequent simulations revealed that a similar network of interactions was established as it is found in the template. The optimized model of the complex is shown in Figure 4a and b. This system is stabilized by hydrophobic forces and also by specific types of cross-helix Cα–H···O hydrogen bonds.[26] Such pairing exists between Gly and Ala residues, and the Ile and Leu residues next in sequence from a complementary helix (Figure 4c). The surface contact area is 4.83 nm^2 (Table 1), and the angle between helices (Figure 4b) is 36°. The closest distance between helices (measured in cross– point between helix centers) is 0.70 nm. We also calculated the interaction energy between two helical fragments (18 residues not containing charged amino acids) in the model to be $-152\ kJ\,mol^{-1}$. This is a signifi-

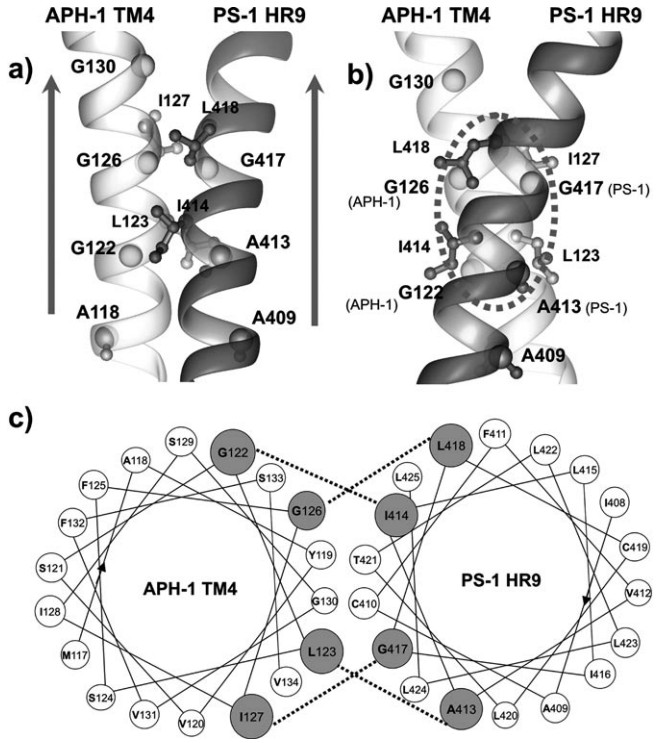

Figure 4. The model Parallel 1 of the interface between APH-1 TM4 and PS-1 HR9 based on the homology to GpA. Cα of Gly and Ala forming the interface are shown as shaded spheres. a) Side view: the thick arrows indicate directions of helices. b) Side view rotated 90°; the dashed ellipse marks the contact area. c) Schematic representation of helix–helix interactions in the model.

Table 1. Comparison of interaction energies and contact surface areas for wild-type and mutant models of the APH-1 TM4–PS-1 HR9 complex.

Model	PS-1 mutation	$E_{interaction}$ [kJ mol^{-1}]	Contact surface area [nm^2]
Parallel 1	wild-type	−152	4.83
Parallel 2	wild-type	−147	4.65
Antiparallel 1	wild-type	−218	4.11
Antiparallel 2	wild-type	−234	4.33
	A409T	−264	4.24
	C410T	−232	4.39
	L418F	−233	4.38
Antiparallel 2 (another conformation)	wild-type	−262	4.39
	A409T	−287	4.26
	C410T	−263	4.37
	L418F	−266	4.46

cantly higher binding energy than the respective value calculated for the GpA dimer (−123 kJ mol^{-1}).

We also examined a second alignment, where the PS-1 HR9 sequence is shifted by four residues. This new alignment also employs the same GxxxG motif on both interacting helices. The contact surface area is slightly smaller, at 4.65 nm^2. The angle between helices and the closest distance between helices are the same as before because the same template was used. The calculated binding energy was less negative, −147 kJ mol^{-1}, so this interaction is also more stable than in the GpA template dimer. In both models (Parallel 1 and Parallel 2) identical types of interaction are present, that is, branched hydrophobic residues (Leu, Ile, Val) face small residues (Gly or Ala). Because of the large angle between helices, the main area of contact in both models involves only one GxxxG motif from each helix. G122 participates in the main contact area in the Parallel 1 model but is outside this area in Parallel1 2.

The alignment score calculated for the Parallel 1 model was 23 for APH-1 TM4 and 24 for PS-1 HR9. For the Parallel 2 model the score was 23 for APH-1 TM4 (the same alignment) and −2 for PS-1 HR9. These scores are in agreement with the interacting energies and contact surfaces, favoring the Parallel 1 model.

Models of the APH-1–PS-1 interface based on AqpM

The investigation of the plausible antiparallel orientation by homology modeling is more difficult because there is no transmembrane dimer with a GxxxG-based interaction between antiparallel helices that could serve as a template. Some clues, however, can be provided by inspection of membrane-embedded protein models found in the RCSB protein data bank (PDB),[27] from which examples of analogous interaction can be drawn. For example, the structure of aquaporin (AqpM, PDB code: 2F2B), resolved by Lee et al. using X-ray diffraction,[28] contains a bundle of six TM helices. Two of these helices (TM2 and TM5) are tightly packed against each other in an antiparallel orientation. Each helix contains a tandem of motifs of two small residues separated by three other residues ((**G**59)LAF**G**FAI(**A**67) and (**G**176)III**G**LTV(**A**184), respectively) and these motifs directly face each other.

The driving force for interactions between helices TM2 and TM5 in AqpM does not result from interactions between adjacent helices but from the motifs of small residues GxxxG. This is apparent from distances between helices. The smallest distance (0.73 nm), indicating the highest interaction binding energy (−327 kJ mol^{-1}), is between helices TM2 and TM5 (Table 2). Other distances are much larger 0.90 and 0.96 nm, between helices TM1–TM2 and TM5–TM4, respectively. Contact surfaces are nearly the same because interfaces with adjacent helices are made of amino acids with larger side chains. The

Table 2. Parameters of the interface between adjacent helices in AqpM.

Interface	$E_{interaction}$ [kJ mol^{-1}]	Contact surface area [nm^2]	Helix–helix distance [nm]	Helix–helix angle [°]
TM1–TM2	−122	4.14	0.90	15
TM2–TM5	−327	4.13	0.73	26
TM5–TM4	−90	4.41	0.96	15

angles between adjacent helices are both small, and account for 15°, also suggesting a lack of tight packing. The GxxxG-based interface in TM2–TM5 is flanked by two hydrogen bonds located within these helices, W55–N192 and Y71–$I177_{(carbonyl)}$, which additionally strengthen this contact and contribute to the interaction energy. No hydrogen bonds were found in the interfaces with adjacent helices. All these findings additionally justify use of the TM2–TM5 pair as a template for protein–protein interactions.

Two alternative models of antiparallel orientation of the interacting helices were built based on the AqpM template. In the first model, termed Antiparallel 1, APH-1 TM4 was aligned with AqpM TM2, and PS-1 HR9 was aligned with AqpM TM5. The Antiparallel 2 model was constructed using swapped template helices (Figure 5). The pattern of interactions between PS-1 HR9 and APH-1 TM4 is quite different from that in previous models. Because the angle between helices is smaller (26°), the contact area is longer but narrower (Figure 6 a and b) and involves the whole GxxxGxxxG motif. Small residues from both helices are arranged linearly and placed alternately. A schematic representation of these interactions is shown in Figure 6 c. Although the whole motif is involved in the interaction, the contact surface is much smaller: in the case of the Antiparallel 1 model, the contact surface is 4.11 nm^2, whereas the respective value for the Antiparallel 2 model is 4.33 nm^2. Additionally the closest distance between helices (measured in cross-point between helix centers) is larger (0.75 nm) than previous models based on the GpA template. The binding energy, however, is much lower for these models than for the two previous models with helices oriented parallel: the binding energy for Antiparallel 1 was $-218\ kJ\,mol^{-1}$, and for Antiparallel 2, $-234\ kJ\,mol^{-1}$ (Table 1).

The alignment scores calculated for the Antiparallel models were smaller than for the Parallel models: for Antiparallel 1, 8 for APH-1 TM4 and 10 for PS-1 HR9; for Parallel 2, 11 for APH-1 TM4 and −5 for PS-1 HR9. Such alignment scores are in contrast to the interacting energies and contact surfaces that favor the Antiparallel 2 model. A negative score comes mainly

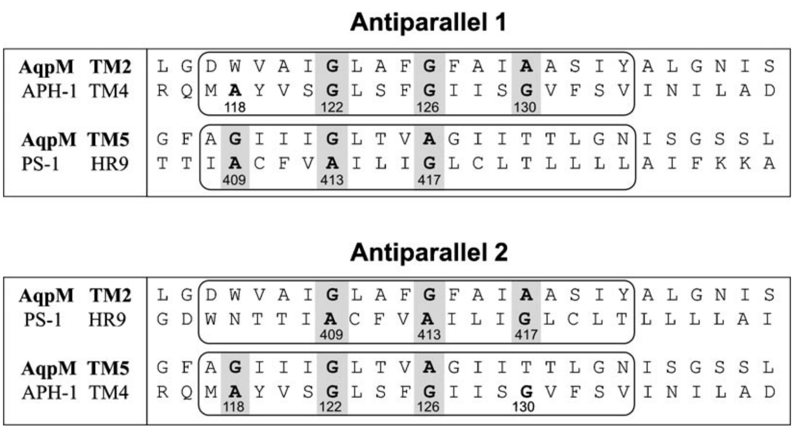

Figure 5. Two alignments of APH-1 TM4 and PS-1 HR9 using the template sequences of TM2 and TM5 helices of AqpM. Rounded squares mark helical sequence areas in the modeled helices. These areas were taken to calculate interaction energies and contact surface areas. Grey boxes denote the most important residues for alignment.

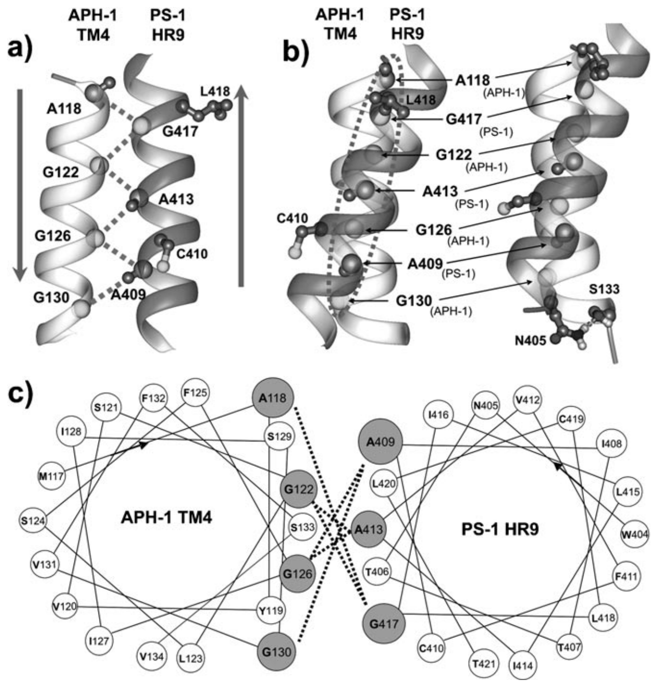

Figure 6. The Antiparallel 2 model of the interface between APH-1 TM4 and PS-1 HR9 based on the homology to AqpM. Cα of Gly and Ala forming the interface are shown as shaded spheres. FAD-related residues, C410 and L418, analyzed for the influence of mutations on the interface are also shown. a) Side view: the thick arrows indicate directions of helices. b) Side view rotated 90°: the dashed ellipse marks the contact area. c) Schematic representation of helix–helix interactions in the model. Because of the large number of interactions, the helical wheels were slightly distorted so that all interactions are clear in the figure.

from the flanking residue pairs in AqpM TM2 and PS-1 HR9 containing Trp residues (Figure 5). Confining the analyzed fragment to 16 instead of 18 residues increases the alignment score from −5 to +6.

In the Antiparallel 2 model alignment, the second 3D structure of the interface is possible because S133 of APH-1 and N405 of PS-1 can form a hydrogen bond. Such additional attraction increases the contact surface (4.39 nm^2) and greatly improves the binding energy ($-262\ kJ\,mol^{-1}$) of interacting helices (Table 1 and Figure 6 b).

Discussion

In the present work, four molecular models of helix–helix interactions in the putative interface between APH-1 and PS-1 were proposed. The spatial distribution of residues along the APH-1 TM4 helix strongly suggests the face of the helix containing three Gly residues forms an interface that is able to interact with another helix within the γ-secretase complex. This agrees with APH-1 topology and that its N-terminus TM4 traverses the membrane from cytoplasm to the extracellular matrix. Two models of interaction based on GpA predict that the direction of PS-1 HR9 should also point from the cytoplasm to the extracellular environment which is in contrast to all pub-

lished topologies of PS-1. The antiparallel orientation of both helices gave rise to two other proposed models of interaction resembling that found in AqpM and formed by a row of small residues.

Molecular biological investigations indicate that the initial assembly of γ-secretase starts from the formation of the sub-complex between APH-1 and NCT independently of the conserved GxxxGxxxG motif of APH-1.[29] On the other hand, it was determined that certain mutations in this motif affect the interactions of the APH-1–NCT sub-complex with presenilin.[19] An important insight into these interactions has been made recently by two independent research groups, suggesting that the APH-1–NCT complex interacts with the C terminus of PS-1 rather than with PS-1 NTF.[30,31] Such an interaction was proposed based on co-immunoprecipitation of APH-1–NCT with PS-1 CTF in partly detergent-solubilized membranes. All these results comply with the notion that the C-terminal region of PS-1 may interact with the GxxxGxxxG motif of APH-1.

All three HRs (8–10) in PS-1 CTF bear the GxxxG motif. However, HR8 directly forms the catalytic site, and HR10, which contains the PAL region, is also recognized as essential for the catalytic activity of γ-secretase. According to Wang et al., HR10 is not involved in the formation or stabilization of the γ-secretase complex.[32,33] The PAL motif is required by other aspartic proteases and most of them do not form a complex with additional proteins for activity.[2] Taking into account the fact that HR8 and HR10 are involved in substrate processing, HR9 seems to be the most plausible one to form an interface for interaction with APH-1 (Figure 7).

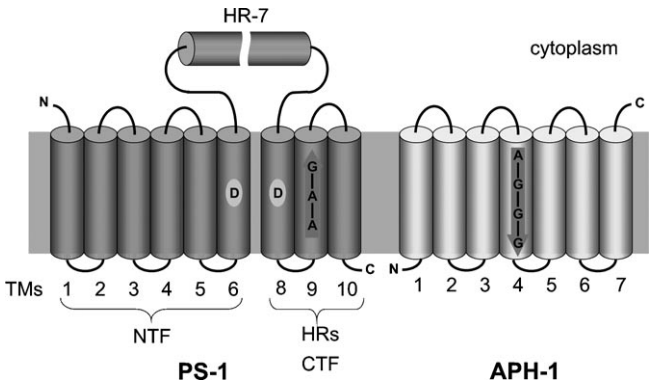

Figure 7. Scheme of topologies of PS-1 and APH-1 with the suggested interface between them highlighted by arrows. The locations of two catalytic aspartic acid residues of PS-1 are also shown.

Genotyping of the APH-1 TM4 fragment in our FAD patients indicated that DNA sequence variation of the fragment does not contribute to familial Alzheimer's disease development. Our data is in agreement with the results presented by Poli et al.,[23] which indicate that sequence variation in any of the two APH genes are not risk factors for SAD in the Italian population. Three out of six different polymorphisms in the *aph1b* gene results in amino acid substitutions (T27I, V199L, and F217L), whereas the others are either silent or in noncoding regions. All amino acid polymorphisms identified by Poli et al. are outside TM4.

Calculated alignment scores are mostly positive, indicating the feasibility of both chosen templates, GpA and AqpM, for comparative modeling. Negative scores obtained for the best model, Antiparallel 2, come from two flanking residue pairs in AqpM TM2 and PS-1 HR9 containing Trp residues (Figure 5). Removal of these pairs by confining the analyzed fragment to 16 residues instead of 18, increased the alignment score from −5 to +6. This effect can also be achieved by introducing a single amino acid gap to align two Trp residues from both sequences. Trp–Trp pair alignment is valued at +17 points in this score. Flanking Trp residues are very important for the proper anchoring of transmembrane helices in the membrane.

In the GpA-based models created, two interacting helices are oriented in parallel (that is, with the same membrane-spanning vector). A lower binding energy obtained for the wild-type (Table 1) suggests that the Parallel 1 model is better (Figure 4a and b). However, the parallel orientation of PS-1 HR9 in relation to APH-1 TM4 is contrary to most of the experimental evidence available so far. Although several topologies of PS-1 are currently debated, most of them assume PS-1 HR9 directs its C-terminal end toward the cytosolic side. Thus, we examined the antiparallel orientation of PS-1 HR9 in relation to APH-1 TM4 and built the respective molecular models.

In antiparallel orientation, the (**A**409)xxx**A**xxx(**G**417) motif located on the PS-1 HR9 helix can interact with an extended (**A**118)xxx**G**xxx**G**xxx(**G**130) motif found in APH-1 TM4. This is because of a much smaller helix–helix angle relative to the parallel models. Paradoxically this extension diminishes the contact surface but also greatly improves the binding energy (Table 1). This strongly suggests that the antiparallel models are a better approximation of the interface. Among them the Antiparallel 2 model is characterized by the lowest binding energy (Figure 6a and b). This energy may be much lower if the additional conformations of the Antiparallel 2 model (Figure 6b) that resulted from our modeling study are taken into consideration. The hydrogen bond between S133 of APH-1 and N405 of PS-1 greatly improves interactions in the model and stabilizes the complex. As was found by Schneider and Engelman[34] in mutational studies of glycophorin A, the motifs of two small residues can assist but are not sufficient for transmembrane helix interactions. The framework of adjacent side chains is essential for creating stable helix interactions, so the case of each (small)xxx(small) motif must be tested independently. In the analyzed PS-1–APH-1 interface there is a long network of small residues (Figure 6a) and a hydrogen bond between interacting helices. Such an arrangement of residues in the Antiparallel 2 model provides the lowest binding energy and the most probable mode of interaction.

The analyzed fragments were confined to 18 residues to exclude all ionic interactions, but such interactions are also very important for a strong interface. In the Parallel models there is a hypothetical possibility of ionic interaction between D140 from APH-1 TM4 and K429 (or K430) from PS-1 HR9. However, taking into account the large angle between interacting helices (36°), the potentially interacting ionic residues are distant

from one another. In the Antiparallel models there are no such attractive ionic interactions of flanking residues. Instead, in the Antiparallel 1 model there is a possibility of a repulsive interaction between K429 (or K430) from PS-1 HR9 and R115 from APH-1 TM4. But in the Antiparallel 2 model there is a possibility of formation of an additional hydrogen bond between D403 from PS-1 HR9 and N136 from APH-1 TM4. Further experimental data are required to reveal all details of the binding of both proteins. Another issue of great importance to the binding is the influence of adjacent helices in both interacting proteins on the interface. Because of short loops between transmembrane helices in PS-1 and especially in APH-1, the binding interface is composed of more than one helix from each protein. However, the driving force for creation of this interface is hydrophobic in nature and, in particular, based on (small)xxx(small) motifs.

In the recent paper by Sato et al.[35] confirms the stoichiometry of γ-secretase components PS-1/PEN-2/nicastrin/APH-1 is 1:1:1:1, and also that APH-1 is present in this complex as a monomer. The (small)xxx(small) motifs present in PS-1 and APH-1 do not lead to dimerization of both proteins separately. This behavior may be due to hiding of these motifs in immature forms of both proteins but also due to repulsive interactions of ionic residues flanking the transmembrane helices containing such motifs in homodimeric interfaces.

The proposed interface fragment of the PS-1 HR9 helix contains three FAD-associated mutations (A409T, C410T, and L418F).[13] The influence of these mutations was assessed by comparison of the binding energies and contact surfaces, and the results are presented in Table 1. Analysis of this data suggests that mutations C410T and L418F introduced into the models have nearly no effect on binding energy, whereas A409T greatly improved this energy (-264 and -287 kJ mol^{-1} for the first and the second Antiparallel 2 conformations, respectively). The rationale behind this is the formation of an additional hydrogen bond between A409T of PS-1 and $G126_{(carbonyl)}$ of APH-1 (the side chain of S129 is also a potential partner). Other mutations are outside the area of the analyzed interface; however, they may influence the PS-1–APH-1 contact by altering interactions with adjacent helices of respective proteins. For analysis of such effects the whole structures of both interacting proteins are needed.

Conclusions

The most negative binding energies calculated for the Antiparallel 2 model as well as its mutants corroborate the most recent studies on membrane topology of the PS-1 molecule. This strongly advocates the antiparallel relation between the APH-1 TM4 and PS-1 HR9 helices. The model containing a GxxxG motif represents the core of the APH-1–PS-1 interface. Analysis of binding energies and contact surfaces of helix–helix interactions suggests that the Antiparallel 2 model is the most probable approximation of the single helix–helix interface between APH-1 and PS-1. The (small)xxx(small) hydrophobic motif would be a driving force for the assembly both proteins. Then additional interactions, like flanking residues forming hydrogen bonds or ionic interactions and adjacent helices from both proteins, would contribute to this interface by modifying and strengthening it. The created model is only the first step for building the whole interface, but it contains the recognition pattern that facilitates the assembly of APH-1 and PS-1. This model can be used in further studies on refinements of the molecular constitution of γ-secretase and its components and possibly for future drug design as well.

Experimental Section

Modeling helix–helix interactions

Homology/comparative modeling was performed based on helix–helix template structures employing GxxxG motifs. We used two TMs from the dimer of glycophorin A (GpA, PDB code: 1AFO) which served as a template for parallel orientations of interacting helices. Another system involving TM2 and TM5 from aquaporin (AqpM, PDB code: 2F2B) was used as a template for antiparallel orientations of interacting helices. The alignments were performed manually based on small-residue motif pairing and maximal overlapping of transmembrane helices. The alignment scores were calculated using PAM250 substitution matrix by summing individual scores from each pair of aligned amino acids. This matrix provides no penalty for Gly/Ala substitution, which is a requirement for modeling (small)xxx(small) interactions.

In the case of the GpA template two alignments were possible with a shift of one target sequence by four residues, so we developed two alternative 3D models of interactions for parallel orientations of interacting helices. In the case of antiparallel orientations two alternative models were built based on swapped TM helices of the template in sequence alignments. Based on these alignments four different models of helix–helix interface (named Parallel 1, Parallel 2 and Antiparallel 1, Antiparallel 2) were developed. The use of a comparative modeling program was not needed because we modeled two separate helices in the interface and we wanted to have full control of the optimization process of such a fragile system. All amino acid substitutions were done manually based on identical location of backbone atoms and identical angles.

For energy refinements, helices in each model were end-capped with acetyl and *N*-methyl groups on their N and C termini, respectively. These helices were trimmed to 18 amino acids to eliminate any charged residues, which may strongly influence calculations of interaction energy between helices. Each model was then subjected to energy minimization in vacuum, first using the steepest descent method and then simulated annealing. In the second method, the temperature was continuously lowered from 300 to 0 K during the molecular dynamics simulation. The simulated annealing was applied in three steps by gradual unfreezing, allowing the motion of 1) hydrogen atoms only, 2) hydrogen + side chain atoms, and 3) all atoms (no constraints).

In order to validate the optimized complexes we calculated the interaction energies defined as the difference between the total energy of the complex and the sum of total energies of two separate helices. We also calculated the contact surface of the interface as a difference between the sum of solvent-accessible surfaces of separated helices and the solvent-accessible surface of the complex divided by two. All calculations were performed in Yasara Dynamics program v. 6.10 (Yasara Biosciences) using the AMBER 99 force field. Yasara is a molecular modeling program for building proteins and small molecules, energy minimization, and molecular

dynamics. Yasara allows for interactive (involving manual dragging) molecular dynamics, which greatly facilitates finding new conformations and exploring the various binding modes. Because of built-in semiempirical procedures, Yasara is also able to calculate the partial atomic charges needed for molecular mechanics and dynamics procedures, for small molecules, and nonstandard residues.

APH-1 TM4 genotyping in patients with FAD

The cohort of 55 unrelated patients with FAD diagnosed in the outpatient clinic of the Department of Neurodegenerative Disorders of the Medical Research Centre of the Polish Academy of Sciences in Warsaw were investigated in the study. All patients were examined by a neurologist, a neuropsychologist, a psychiatrist, and had a CT scan of the brain. The diagnosis of AD was confirmed using a standardized protocol according to the National Institute of Neurological and Communicative Disorders and Stroke–Alzheimer's Disease and Related Disorders Association (NINCDS-ADRDA). FAD was diagnosed if at least one additional first-degree relative suffered from dementia. Written consent was obtained from all participants or their relatives. The study was approved by the Ethics Committee of the MSWiA Hospital in Warsaw.

Genomic DNA was isolated from whole blood by salting out. The polymerase chain reaction (PCR) was performed in a volume of 25 μL with Qiagen Taq PCR Master Mix (2.5 U Taq DNA polymerase, 1× Qiagen PCR buffer containing 1.5 mM $MgCl_2$, 200 μM each dNTP) and primers (20 pmol each). Amplified fragment, which corresponds to the fourth transmembrane domain (TM4) in the APH-1a protein, encompasses a part of exon 3, intron 3, and a part of exon 4 of the APH-1a gene sequence. Sequencing PCR was performed in a volume of 10 μL with the ABI PRISM Big Dye Terminator v1.1 Cycle Sequencing Kit. The direct sequencing was performed on ABI PRISM 310.

Acknowledgements

The work was supported by the Polish Ministry of Science and Higher Education (Grant No: 2P05A 12929) to K.J. K.J. and L.B. thank the Foundation for Polish Science for fellowships supporting their research. We thank C. Zekanowski for critical reading of the manuscript.

Keywords: γ-secretase · GxxxG motif · molecular modeling · molecular recognition · presenilin

[1] A. L. Brunkan, A. M. Goate, *J. Neurochem.* **2005**, *93*, 769–792.
[2] B. Martoglio, T. E. Golde, *Hum. Mol. Genet.* **2003**, *12*, 201R–206R.
[3] M. P. Mattson, *Nature* **2004**, *430*, 631–639.
[4] G. Evin, L. D. Canterford, D. E. Hoke, R. A. Sharples, J. G. Culvenor, C. L. Masters, *Biochemistry* **2005**, *44*, 4332–4341.
[5] D. Edbauer, E. Winkler, J. T. Regula, B. Pesold, H. Steiner, C. Haass, *Nat. Cell Biol.* **2003**, *5*, 486–488.
[6] W. T. Kimberly, M. J. LaVoie, B. L. Ostaszewski, W. Ye, M. S. Wolfe, D. J. Selkoe, *Proc. Natl. Acad. Sci. USA* **2003**, *100*, 6382–6387.
[7] N. Takasugi, T. Tomita, I. Hayashi, M. Tsuruoka, M. Niimura, Y. Takahashi, G. Thinakaran, T. Iwatsubo, *Nature* **2003**, *422*, 438–441.
[8] F. S. Chen, H. Hasegawa, G. Schmitt-Ulms, T. Kawarai, C. Bohm, T. Katayama, Y. J. Gu, N. Sanjo, M. Glista, E. Rogaeva, Y. Wakutani, R. Pardossi-Piquard, X. Y. Ruan, A. Tandon, F. Checler, P. Marambaud, K. Hansen, D. Westaway, P. St George-Hyslop, P. Fraser, *Nature* **2006**, *440*, 1208–1212.
[9] V. A. Morais, A. S. Crystal, D. S. Pijak, D. Carlin, J. Costa, V. M. Y. Lee, R. W. Doms, *J. Biol. Chem.* **2003**, *278*, 43284–43291.
[10] C. Zekanowski, M. P. Golan, K. A. Krzysko, W. Lipczynska-Lojkowska, S. Filipek, A. Kowalska, G. Rossa, B. Peplonska, M. Styczynska, A. Maruszak, D. Religa, M. Wender, J. Kulczycki, M. Barcikowska, J. Kuznicki, *Exp. Neurol.* **2006**, *200*, 82–88.
[11] A. Tandon, E. Rogaeva, M. Mullan, P. H. St George-Hyslop, *Curr. Opin. Neurobiol.* **2000**, *13*, 377–384.
[12] J. Hardy, R. Crook, *Neurosci. Lett.* **2001**, *306*, 203–205.
[13] K. Jozwiak, C. Zekanowski, S. Filipek, *J. Neurochem.* **2006**, *98*, 1560–1572.
[14] J. Kim, R. Schekman, *Proc. Natl. Acad. Sci. USA* **2004**, *101*, 905–906.
[15] A. Henricson, L. Kall, E. L. Sonnhammer, *FEBS J.* **2005**, *272*, 2727–2733.
[16] H. Laudon, E. M. Hansson, K. Melen, A. Bergman, M. R. Farmery, B. Winblad, U. Lendahl, G. von Heijne, J. Naslund, *J. Biol. Chem.* **2005**, *280*, 35352–35360.
[17] D. Spasic, A. Tolia, K. Dillen, V. Baert, B. De Strooper, S. Vrijens, W. Annaert, *J. Biol. Chem.* **2006**, *281*, 26569–26577.
[18] R. R. Fortna, A. S. Crystal, V. A. Morais, D. S. Pijak, V. M. Y. Lee, R. W. Doms, *J. Biol. Chem.* **2003**, *279*, 3685–3693.
[19] M. Niimura, N. Isoo, N. Takasugi, M. Tsuruoka, K. Ui-Tei, K. Saigo, Y. Morohashi, T. Tomita, T. Iwatsubo, *J. Biol. Chem.* **2004**, *280*, 12967–12975.
[20] C. Goutte, M. Tsunozaki, V. A. Hale, J. R. Priess, *Proc. Natl. Acad. Sci. USA* **2002**, *99*, 775–779.
[21] D. Edbauer, C. Kaether, H. Steiner, C. Haass, *J. Biol. Chem.* **2004**, *279*, 37311–37315.
[22] S. F. Lee, S. Shah, C. Yu, W. C. Wigley, H. Li, M. Lim, K. Pedersen, W. Han, P. Thomas, J. Lundkvist, Y. H. Hao, G. Yu, *J. Biol. Chem.* **2003**, *279*, 4144–4152.
[23] M. Poli, L. B. Gatta, S. Archetti, A. Padovani, A. Albertini, D. Finazzi, *Neurosci. Lett.* **2003**, *350*, 77–80.
[24] A. Senes, D. E. Engel, W. F. DeGrado, *Curr. Opin. Struct. Biol.* **2004**, *14*, 465–479.
[25] K. R. MacKenzie, J. H. Prestegard, D. M. Engelman, *Science* **1997**, *276*, 131–133.
[26] A. R. Curran, D. M. Engelman, *Curr. Opin. Struct. Biol.* **2003**, *13*, 412–417.
[27] H. M. Berman, J. Westbrook, Z. Feng, G. Gilliland, T. N. Bhat, H. Weissig, I. N. Shindyalov, P. E. Bourne, *Nucleic Acids Res.* **2000**, *28*, 235–242.
[28] J. K. Lee, D. Kozono, J. Remis, Y. Kitagawa, P. Agre, R. M. Stroud, *Proc. Natl. Acad. Sci. USA* **2005**, *102*, 18932–18937.
[29] M. J. LaVoie, P. C. Fraering, B. L. Ostaszewski, W. J. Ye, W. T. Kimberly, M. S. Wolfe, D. J. Selkoe, *J. Biol. Chem.* **2003**, *278*, 37213–37222.
[30] A. Bergman, H. Laudon, B. Winblad, J. Lundkvist, J. Naslund, *J. Biol. Chem.* **2004**, *279*, 45564–45572.
[31] P. C. Fraering, M. J. LaVoie, W. J. Ye, B. L. Ostaszewski, W. T. Kimberly, D. J. Selkoe, M. S. Wolfe, *Biochemistry* **2004**, *43*, 323–333.
[32] J. Wang, A. L. Brunkan, S. Hecimovic, E. Walker, A. Goate, *Neurobiol. Dis.* **2004**, *15*, 654–666.
[33] J. Wang, D. Beher, A. C. Nyborg, M. S. Shearman, T. E. Golde, A. Goate, *J. Neurochem.* **2006**, *96*, 218–227.
[34] D. Schneider, D. M. Engelman, *J. Mol. Biol.* **2004**, *343*, 799–804.
[35] T. Sato, T. S. Diehl, S. Narayanan, S. Funamoto, Y. Ihara, B. De Strooper, H. Steiner, C. Haass, M. S. Wolfe, *J. Biol. Chem.* **2007**, DOI: 10.1074/jbc.M705248200.
[36] S. Jaysinghe, K. Hristova, W. Wimley, C. Snider, S. H. White, http://blanco.biomol.uci.edu/mpex/, **2006**; last accessed November 12, 2007.

Received: July 31, 2007
Revised: October 17, 2007
Published online on December 5, 2007

